Available online at www.sciencedirect.com
ScienceDirect
International Journal of Thermal Sciences 45 (2006) 1127–1139
International Journal of Thermal Sciences
www.elsevier.com/locate/ijts

Comparison between Kim, Wiscombe and least squares scattering phase function renormalization methods

Habib Farhat [a,*], Naziha Abdallah [a], Mohamed Naceur Borjini [b], Rachid Méchi [a], Rachid Saïd [a]

[a] *Laboratoire des Etudes des Milieux Ionisés et Réactifs, IPEIM 5019, Tunisia*
[b] *Faculté des Sciences de Monastir, 5019 Monastir, Tunisia*

Received 7 January 2005; received in revised form 30 October 2005; accepted 6 January 2006

Available online 11 July 2006

Abstract

A numerical code is made allowing the simulation, in two-dimensional geometry, of the radiative transfer within a semi-transparent medium (STM), gray, absorbing, emitting and anisotropically scattering. The solution method is provided by a new formulation of the modified discrete transfer (MDT) method. A bilinear interpolation of the temperature as well as of the scattered radiation intensity within a grid mesh proved to be necessary in order to cure the occurring problem of negative radiation intensities when one calls upon the linear profile of Cumber with a first fine netting. When analysing the effect of the renormalization methods of the scattering phase function of Kim, of Wiscombe and of least squares on the global modeling of radiative transfer in an anisotropic scattering STM, we have shown that the method of Kim is easy to implement and present the same accuracy degree than the one of Wiscombe. However, the technique of least squares offers real prospects since it stands out by the absence of unrealistic values on the diagonal of the matrix associated to the renormalized phase function and the renormalization of the scattering phase function with the desired precision.

Keywords: Phase function; Mie-scattering; Renormalization; Kim; Wiscombe; Least squares; Radiative transfer; Two-dimensional; MDT method; Bilinear interpolation

1. Introduction

In the industrial processes carried at high temperatures such as boilers and incinerators, radiation is regarded as a significant heat transfer mode, even a dominating one. In general, these processes contain a semi-transparent medium (STM), emitting, absorbing and anisotropic scattering due to the production of soot particles (reactive medium). Such applications need a rigorous, reliable and computationally efficient solution method to provide sufficiently accurate radiative heat transfer predictions. In the last decade, various interesting improvements have been achieved in this way such us the development of new spatial differencing schemes [1,2], the circumvention of the ray effect and false scattering [3–6], of the occurring unrealistic negative intensities [5] and the discrete ordinates representation of the scattered radiation to ensure energy conservation [7].

Among the solution methods of the radiation transport equation is the modified discrete transfer (MDT) method performed by Farhat and Radhouani and successfully applied to the case of a parallelepipedic enclosure [8]. In the present investigation, an improved MDT method is proposed in order to solve the radiative transfer equation (RTE) in a two-dimensional rectangular enclosure where anisotropic scattering in a STM is taken into account. In [8] we have adopted the Cumber linear profile [9] which has been applied to temperature (anisothermal grid cells) and scattered radiation, in the same direction of propagation, in each grid cell. The accuracy of the MDT solutions increases when using a coarser first netting near the walls. The Cumber linear profile caused negative radiant intensities when this condition is satisfied. This negativity was not observed when considering a 3-D rectangular enclosure [8]. A bi-linear interpolation method (Fig. 1) is an alternative that enables to assess

* Corresponding author.
E-mail addresses: farhat_ipeim@yahoo.fr (H. Farhat), naziha.abdallah@ipeim.rnu.tn (N. Abdallah), naceur.borjini@fsm.rnu.tn (M.N. Borjini), rachid.mechi@ipeim.rnu.tn (R. Méchi), said@ipeis.rnu.tn (R. Saïd).

1290-0729/$ – see front matter
doi:10.1016/j.ijthermalsci.2006.01.001

Nomenclature

C_{xy}	direction-shape parameter, $= \frac{\eta \Delta y}{\xi \Delta x}$	
d	particle diameter	m
I	radiative intensity	$\mathrm{W\,m^{-2}\,sr^{-1}}$
I^b	blackbody radiant intensity	$\mathrm{W\,m^{-2}\,sr^{-1}}$
L	Lagrangian (Eq. (21))	
n	order of the MDT method	
n'	refractive index	
N_d	total number of ordinate directions, $= n(n+2)/2$	
q	radiative heat flux	$\mathrm{W\,m^{-2}}$
Q	total radiative surface heat flux	W
s	distance coordinate	m
s''	integration variable	m
T	temperature	K
u, v	spatial interpolation coefficients	
w	angular weights	sr
x'	particle size parameter $= \pi d \nu$	
x_{ij}	original estimate of an element of $[x]$	
x^*_{ij}	adjusted value of x_{ij}	
x, y, z	Cartesian coordinates	m
X, Y	dimensions of the enclosure	m
W_{ij}	arbitrary weights	

Greek symbols

Ω	solid angle	sr
$\vec{\Omega}$	ray direction	
$\mathrm{d}\Omega$	differential solid angle around $\vec{\Omega}$	sr
η, ξ, μ	direction cosines	
Δs	distance travelled by a ray in a grid cell	m
$\Delta x, \Delta y, \Delta z$	dimensions of a grid cell	m
ν	wave number	$\mathrm{cm^{-1}}$
λ	Lagrange multiplier	
κ	absorption coefficient	$\mathrm{m^{-1}}$
α	phase function correction coefficient	
β	extinction coefficient, $= \kappa + \sigma_s$	$\mathrm{m^{-1}}$
σ_s	scattering coefficient	$\mathrm{m^{-1}}$
σ	Stefan–Boltzmann constant, $= 5.669 \times 10^{-8} \mathrm{W\,m^{-2}\,K^{-4}}$	
ω	scattering albedo, $= \sigma_s/\beta$	
ε	wall emissivity	
ρ	wall reflectivity, $= 1 - \varepsilon$	
Φ	scattering phase function	
Φ^*	renormalized scattering phase function	
ψ	scattering angle	rd
θ, φ	polar and azimuthal angles, respectively	rd
χ	convergence criterion of the Lagrange multipliers	
$\tau(s_1 \to s_2)$	transmissivity for a $s_1 s_2$ column, $= \exp[-\int_{s_1}^{s_2} \beta(s'')\,\mathrm{d}s'']$	

Subscripts

i	incoming ordinate direction
j	outgoing ordinate direction
$n, n+1$	entry and exit points of a ray crossing a grid cell
w	wall

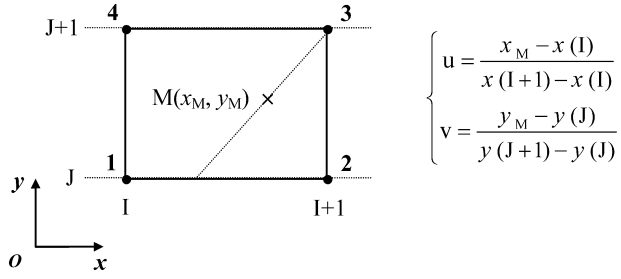

Fig. 1. Definition of the bilinear interpolation of radiant intensity at point M in terms of the neighbouring intensities.

temperature and radiant intensity in any point of a grid cell and to avoid non-physical results. This method could easily be extended to the case of a parallelepipedic configuration.

The scattering phenomenon is represented by a phase function defined as the probability for a radiation beam to be scattered in the propagation direction. To preserve radiant energy conservation, this function must be normalized. Several studies were conducted aiming at the modeling of the radiative properties of the scattering particles by using assumptions among which those related to the size parameter ($x' = \pi\, d\nu$). The Rayleigh approximation is applied for small size parameter and the geometrical optics approximation for a large size parameter. The angular distribution of the scattered radiation in the case of a spherical particle size comparable with the wavelength ($x' \approx 1$) was considered by Mie where the scattering phase function is expressed as a finite series of Legendre polynomials [7,10–12]. The expansion coefficients of the F0 function were given by Lee and Buckius [13] whereas those corresponding to the functions F1, F2 and F3 result from the work of Wiscombe based on the modified code of Mie for size parameters equal to 5, 2 and 1, respectively. The coefficients of the function B1 were given by Özisik [14] for a unit size parameter whereas those of B2 correspond to the angular distribution of radiation scattered by very fine particles [15]. Function F4 is characterised by the same coefficients as function B2, except for a minus sign. Fig. 2 shows the representation of the logarithmic values of the general Mie-anisotropic phase functions studied in this paper. By examining these phase functions, plotted in polar co-ordinates, we can conclude that a weak size parameter presents a more uniform phase function. If this parameter increases, the phase function starts showing scattering peaks in certain directions. Further details about the Mie-scattering phase functions can be found in the references [10–12,16].

A literature survey reveals that any anisotropic scattering phase function could be scaled into isotropic scattering by using the following scaled extinction coefficient and albedo:

$$\widehat{\beta} = \beta(1 - \omega f), \qquad \widehat{\omega} = \frac{\omega(1-f)}{1-\omega f} \tag{1}$$

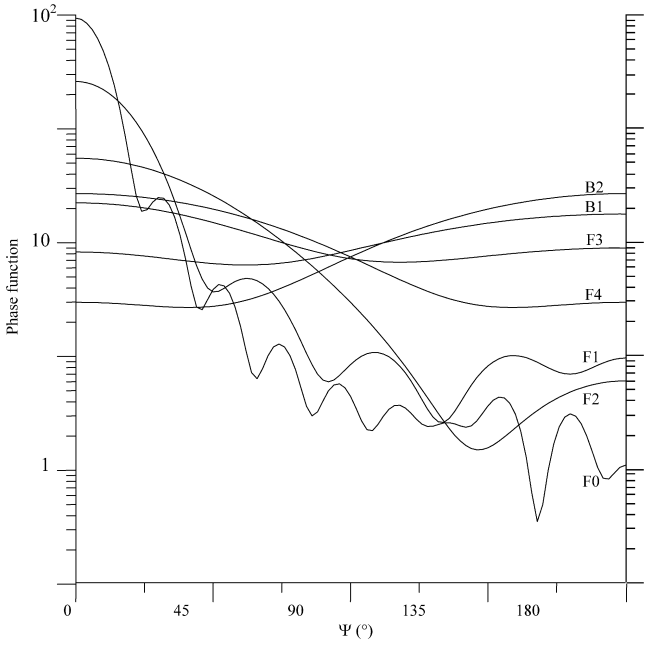

Fig. 2. Representation of the scattering Mie-anisotropic phase functions.

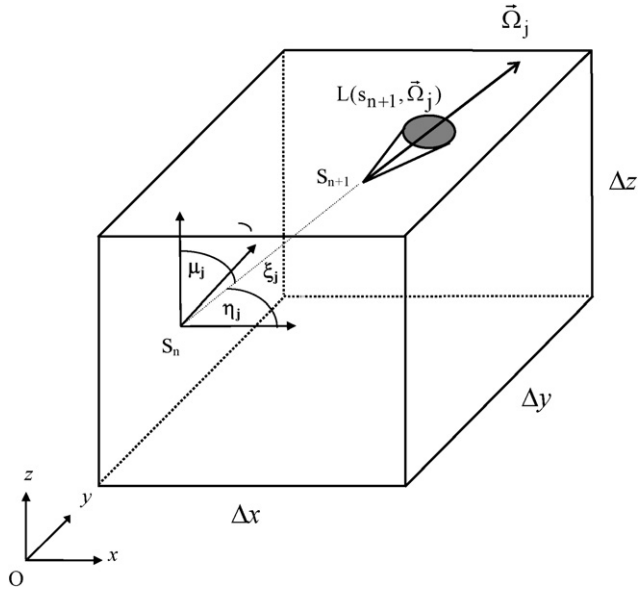

Fig. 3. Representation of a grid cell crossed by a ray in the $\vec{\Omega}_j$ direction.

where $f = \frac{C_1}{3}$ represents the asymmetry factor and C_1 the first order expansion coefficient depending upon the refractive index and the particle form size (Table 1). Tagne and Baillis [17] have derived the above scaled parameters for general anisotropic scattering without assumption on the solution method of the RTE by evaluating the zero and first moments of the scaled albedo and phase function product. These scaled parameters have been previously obtained from the P1 [13] and the delta approximations [18–20]. The isotropic scaling models allow to simplify the anisotropic scattering problem and to reduce the amount of computing time and storage.

The aim of this work is to adapt the least squares method to the renormalization of the scattering phase function. The results of this method are compared to those proposed initially by Kim [10,11] and Wiscombe [15] by conducting modeling of radiative transfer in a rectangular slab having black walls submitted to prescribed temperatures. The medium is a material, gray, absorbing, emitting and anisotropically scattering. In this work, we set out to choose, for the MDT method, the direction set of the DOM of Truelove [21]. The angular representation of the phase functions, which represent the object of this study, are those considered by Mie: F0, F1, F2, F3 and F4 (forward–scattering), B1 and B2 (backward–scattering). A discussion on a better renormalization method of the phase function is given and an evaluation of the accuracy of the scaled isotropic results is made by comparison with available data.

2. Governing equations

When considering the definite solution of the radiative transfer equation (RTE) [22] between two adjacent points s_n and s_{n+1} located respectively at the entrance and exit of a grid cell (Fig. 3), where radiative properties are assumed to be constant, we obtain the equation that governs the radiative transfer within a semi-transparent, gray, absorbing, emitting and anisotropically scattering medium

$$I(s_{n+1}) = I(s_n)\tau(s_n \to s_{n+1}) + \frac{n'^2\sigma\beta(1-\omega)}{\pi}\int_{s_n}^{s_{n+1}} T^4(s'')\tau(s'' \to s_{n+1})\,\mathrm{d}s'' + D(s_{n+1}) \quad (2)$$

with

$$D(s_{n+1}) = \frac{\beta\omega}{4\pi}\int_{s_n}^{s_{n+1}}\left[\int_{\Omega'=4\pi}\Phi(\vec{\Omega}' \to \vec{\Omega})I(s'', \vec{\Omega}')\,\mathrm{d}\Omega'\right] \times \tau(s'' \to s_{n+1})\,\mathrm{d}s'' \quad (3)$$

Table 1
Maximum percentage error between the hot wall radiative flux values obtained by the least squares, Wiscombe, scaled isotropic methods and S14 approximation

	$f = C_1/3$	Least-wis.	Least-scaled	Least-S14	Wis.-scaled	Wis.-S14	Scaled-S14
B1	−0.18841	0.14	1.4	1.1	1.6	1.2	0.37
B2	−0.40000	0.57	2.2	0.91	2.8	1.5	1.3
F0	0.92732	1.4	0.51		1.9		
F1	0.84534	2.3	0.83	0.33	3.2	2.7	0.50
F2	0.66972	6.2	1.5	0.60	7.8	5.6	2.1
F3	0.18452	0.38	0.036		0.34		
F4	0.40000	0.66	1.8		2.5		

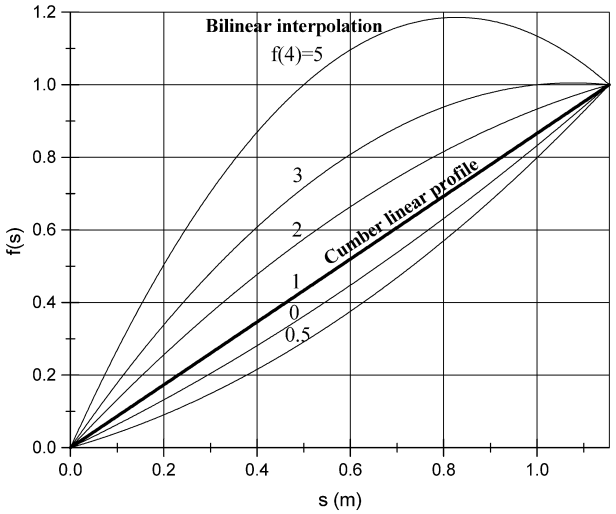

Fig. 4. An illustrative example to compare linear and bilinear interpolation schemes ($f(1) = f(2) = 0$, $f(3) = 1$, $\Delta x = \Delta y = 1$ m).

The discretized form of the integral term of Eq. (3) is

$$D_j(s_{n+1}) = \frac{\beta\omega}{4\pi} \int_{s_n}^{s_{n+1}} J_j(s'')\tau(s'' \to s_{n+1})\,\mathrm{d}s'' \tag{4}$$

where the in-scatter term can be expressed as

$$J_j(s) = \sum_{i=1}^{N_d} I_i(s)\Phi_{i\to j} w_i \tag{5}$$

In a parallelepipedic enclosure, the appliance of the Cumber linear profile [9] on temperature T and scattered radiation J_m, which appears in the definite solution of the RTE, allows us to set up a new equation of radiant intensity transfer [8]. According to this profile, the considered function (T or J_m) is assumed to vary linearly between the entry (s_n) and exit (s_{n+1}) points of a ray traversing a grid cell. More accurate representation of the temperature and the scattered radiation fields within a grid cell should produce more accurate numerical simulations. This is due to the non-linear dependance of the intensity on the temperature. In a two-dimensional configuration, a bi-linear interpolation is an alternative that allows approaching these quantities (T and J_m) in a given point $M(x, y)$ within a grid cell in accordance with those defined in the neighbouring nodes. The evaluation of the integral terms in Eqs. (2)–(3) is carried out, with the desired accuracy, using a trapezoidal method connected to the Romberg convergence speeding up algorithm [23]. Comparison between the Cumber linear profile and the bilinear interpolation scheme (Eq. (30)) for a simplified case is shown in Fig. 4. The discrepancy between the two profiles increases as the considered function value at node 4 (discarded by the Cumber profile) increases. This situation occurs near the wall surfaces of engineering devices carried at high temperatures. In the following section, a bi-linear variation law of the temperature, as well as the scattered radiant intensity, is adopted to show that this approach is effective in simulating the radiative heat transfer in a participating medium.

The discretized radiative boundary condition at the lower part of the medium for example is given as

$$\text{at } y = 0: \quad I_j(S_w) = \varepsilon_w I^b(S_w) + \frac{\rho_w}{\pi} \sum_{(\xi_i<0)} I_i(S_w)|\xi_i| w_i \quad (\xi_j > 0) \tag{6}$$

The x- and y-components of the radiative flux density and the radiative source term, required for the energy equation and obtained by integrating the RTE over the N_d ordinate directions, are expressed respectively as

$$q_{r_x}(s) = \sum_{j=1}^{N_d} I_j(s)\eta_j w_j \tag{7}$$

$$q_{r_y}(s) = \sum_{j=1}^{N_d} I_j(s)\xi_j w_j \tag{8}$$

$$-\vec{\nabla}.\vec{q}_r(s) = (1-\omega)\beta\left[\sum_{j=1}^{N_d} I_j(s)w_j - 4n'^2\sigma T^4(s)\right] \tag{9}$$

When the medium is at the radiative equilibrium, stationary energy conservation is given by

$$4n'^2\sigma T^4(s) = \sum_{j=1}^{N_d} I_j(s)w_j \tag{10}$$

3. Renormalization phase function methods

In the case of scattering particles composed of a homogeneous and isotropic material and presenting a perfect spherical symmetry and/or when the medium does not present preferential scattering directions, the phase function depends only on the scattering angle Ψ evaluated between incidental and scattering directions, thus verifying the following equations:

$$\begin{cases} \Phi(\vec{\Omega}_i, \vec{\Omega}_j) = \Phi(\vec{\Omega}_j, \vec{\Omega}_i) \\ \Phi(-\vec{\Omega}_i, \vec{\Omega}_j) = \Phi(-\vec{\Omega}_j, \vec{\Omega}_i) \end{cases} \tag{11}$$

Taking account of the angular dependence of the radiant intensity and in order to facilitate the numerical resolution of the radiative transfer equation (RTE), the spherical angle is subdivided into N_d elementary solid angles. To each ordinate direction $\vec{\Omega}(\eta, \xi, \mu)$, is associated an angular weight w that represents the area surrounding this direction on the unit radius sphere.

Conservation of radiant energy dictates the following condition:

$$\frac{1}{4\pi} \int_{\Omega'=4\pi} \Phi(\vec{\Omega}', \vec{\Omega})\,\mathrm{d}\Omega' = 1 \tag{12}$$

Due to the difficulty of handling this equation we set out to replace it by a quadrature sum over all the ordinate directions:

$$\frac{1}{4\pi} \sum_{i=1}^{N_d} \Phi_{i,j}(\cos\psi_{i,j}) w_i = 1 \tag{13}$$

This practice involves discretization errors and the scattering phase function is no more normalized. In addition to the methods of Kim and Wiscombe, we propose in this work to adapt the least squares method to the renormalization of the scattering phase function.

3.1. Wiscombe method

This method was initially proposed by Wiscombe [15]. Since the phase function Φ_{ij} puts into play two directions, the author associated to each direction $\vec{\Omega}_i$ a correction factor α_i:

$$\Phi^*_{i,j} = (1+\alpha_i+\alpha_j)\Phi_{i,j} \tag{14}$$

Eq. (13) becomes:

$$\frac{1}{4\pi}\sum_{i=1}^{N_d}(1+\alpha_i+\alpha_j)\Phi_{i,j}w_i = 1 \tag{15}$$

The resulting set of the correction coefficients is provided by solving a system of algebraic equations, which arises in the following matrix form:

$$[A]\{X\} = \{B\} \tag{16}$$

with

$$\begin{cases} X = (\alpha_i)_{i=1,\ldots,N} \\ (A_{i,j})_{i,j=1,\ldots,N_d} = \Phi_{i,j}w_i + \sum_{k=1}^{N_d}\Phi_{k,j}w_k \\ (B_j)_{j=1,\ldots,N_d} = 4\pi - \sum_{k=1}^{N_d}\Phi_{k,j}w_k \end{cases} \tag{17}$$

3.2. Kim technique

This method, adopted by several researchers [8,10,11], is easier to implement than the previous one since it associates a single correction factor depending only on the scattering direction $\vec{\Omega}_j$ yielding:

$$\Phi^*_{i,j} = \frac{\Phi_{i,j}}{\frac{1}{4\pi}\sum_{k=1}^{N_d}\Phi_{k,j}w_k} \tag{18}$$

To be able to compare the values of the correction coefficients obtained by the two methods of Wiscombe and Kim, it is advisable to use the same form for the renormalized phase function $\Phi^*_{i,j}$ as follows:

$$\Phi^*_{i,j} = (1+2\alpha_j)\Phi_{i,j}$$
$$\alpha_j = \frac{1}{2}\left[\frac{1}{\frac{1}{4\pi}\sum_{k=1}^{N_d}\Phi_{k,j}w_k} - 1\right] \tag{19}$$

3.3. Least squares method

Larsen and Howell [24], then Méchi et al. [25] applied this method to normalize the direct exchange areas in zonal analysis which embody the enclosure's optical and geometric properties [26,27]. Ou and Wu [7] have performed this method for inverse radiation problems in conjunction with the Levenberg–Marquardt algorithm. Its application consists in adjusting the original estimates $x_{i,j} = \Phi_{i,j}w_i$ $(i,j = 1,\ldots,N_d)$ with the following constraints to ensure radiant energy conservation:

$$\begin{cases} \sum_{i=1}^{N_d} x_{i,j} = c_j \\ c_j = 4\pi, \quad j = 1,\ldots,N_d \end{cases} \tag{20}$$

According to Larsen and Howell [24], this problem consists in minimizing the Lagrangian L defined by:

$$L = H + \sum_{j=1}^{N_d}\lambda_j(g_j + g^*_j) \tag{21}$$

where

$$\begin{cases} H = \sum_{i=1}^{N_d}\sum_{j=1}^{N_d}\frac{1}{2W_{i,j}}(x^*_{i,j} - x_{i,j})^2 \\ g_j = c_j - \sum_{i=1}^{N_d}x^*_{j,i}, \quad j = 1,\ldots,N_d \\ g^*_j = c_j - \sum_{i=1}^{N_d}x^*_{i,j}, \quad j = 1,\ldots,N_d \end{cases} \tag{22}$$

Notice that $x_{i,j}$ and $x^*_{i,j}$ represent the original estimate and the adjusted value of an element of $[x]$. $W_{i,j}$ are the selected coefficients chosen in such a way that they preserve the symmetry of the matrix associated to the renormalized phase function $(W_{ij} = W_{ji})$.

The Lagrange multipliers λ_i are calculated following the resolution of a system of algebraic equations, obtained by minimizing the Lagrangian L with respect to each value $x^*_{i,j}$:

$$\frac{\partial L}{\partial x^*_{i,j}} = \frac{1}{W_{i,j}}(x^*_{i,j} - x_{i,j}) - \lambda_i - \lambda_j = 0$$
$$i,j = 1,\ldots,N_d \tag{23}$$

This equation results in:

$$x^*_{i,j} = x_{i,j} + W_{i,j}(\lambda_i + \lambda_j), \quad i,j = 1,\ldots,N_d \tag{24}$$

Taking account of the radiative energy conservation constraints (Eq. (20)), the summation of this equation on the total discrete directions yields:

$$4\pi - \sum_{i=1}^{N_d}x_{i,j} = \sum_{i=1}^{N_d}W_{i,j}(\lambda_i + \lambda_j), \quad j = 1,\ldots,N_d \tag{25}$$

The determination of the Lagrange multipliers consists in solving an algebraic system of N_d equations and the resulting equations may be written in the following matrix form:

$$[R]\{\lambda\} = \{\delta\} \tag{26}$$

with

$$\begin{cases} r_{i,i} = W_{i,i} + \sum_{j=1}^{N_d}W_{j,i} \\ r_{i,j} = W_{i,j}, \quad i \neq j \\ \delta_j = 4\pi - \sum_{i=1}^{N_d}x_{i,j} \end{cases} \tag{27}$$

The computation process of the Lagrange multipliers is repeated checking the following convergence condition:

$$\sum_{i=1}^{N_d}\left(\lambda_i^p - \lambda_i^{p-1}\right)^2 < \chi \tag{28}$$

The values of the renormalized phase function are deduced using Eq. (24).

3.4. Results and discussion

The numerical results, obtained by applying the renormalization methods of Kim, Wiscombe and least squares, correspond to the quadrature order sets ranging from 2 (4 directions) to 12 (84 directions) and to the Mie-phase functions (B1, B2, F0, F1, F2, F3 and F4). The total solid angle 4π sr is discretized into $N_d = n(n+2)/2$ infinitesimal fully-symmetrical control angles (2-D analysis) with ensuring invariance properties of the physical system [28]. The used quadrature set obeys the intensity distribution moments of order 1 (half-range), to ensure realistic boundary heat fluxes and temperatures, and of orders 0 and 2 (full-range) [21,29–31].

For a given angular quadrature set and a given phase function, the average percent error is evaluated using the three methods adopted in the present work:

$$\%\ \text{average error} = \frac{1}{N_d}\sum_{j=1}^{N_d}(\%\ \text{error})_j = \frac{1}{N_d}\sum_{j=1}^{N_d}\left|1-\frac{1}{4\pi}\sum_{i=1}^{N_d}\Phi^*_{i,j}w_i\right|\times 100 \qquad (29)$$

By examining the obtained percentage errors, we can state that without renormalization, the introduced error is generally significant reaching up to 2.3 10^3% and that the increase of the quadrature order does not decrease it (Fig. 5). This makes it necessary to renormalize the phase function in order to avoid the non-physical encountered results and to enhance the accuracy of the in-scattering contribution when checking the RTE solution in radiating enclosures. The average error highest values correspond to the really acute Mie-phase functions F0 and F1. This can be explained by the large forward scattered component present in each function and the important number of expansion coefficients assigned to these phase functions provided in [10,11].

For all the quadrature sets used ($n = 2, \ldots, 12$) the average errors obtained by the Kim [8,10,11] and Wiscombe [15] methods are quite satisfied (about 10^{-14}). In addition, for $n > 4$ and $\chi = 10^{-15}$ the least squares technique led to less average errors. The results of the former can be accomplished with the required accuracy when improving the accuracy of the Lagrange multipliers (Eq. (28)). By applying Kim's method, Kim and Lee [10] have shown that the phase functions B1, B2 and F2 normalize to less than 0.1% when using the S14 approximation whereas for the Mie-function F1 the average renormalization error is 1.4576%. By comparison with our results (Kim's method), the difference could be explained by the fact that the moment matching quadrature scheme adopted in the present work was different from the one used in the above reference. Tests have shown that $W_{i,j} = w_i$ was a judicious choice allowing, on the one hand, to preserve the symmetry of the matrix associated to the renormalized phase function and, on the other, to tackle the drawback of the unrealistic values of the phase function occurring when the incident direction corresponds to the scattering one ($\Psi_{i,i} = 0$): In fact, the values $\Phi^*_{i,i}$ placed on the diagonal of the matrix $[\Phi^*]$ obtained by this technique are identical, which concords with the basic assumption that $\Phi_{i,j}$ depends only on the scattering angle $\Psi_{i,j}$. Indeed, the difference between the values occupying the diagonal of the matrix $[\Phi^*]$ reproduced by the methods of Wiscombe and Kim was predictable according to Eqs. (14) and (19). It is to be noted that the numerical computer code is sufficiently flexible to treat the case of other phase functions not under consideration in this work.

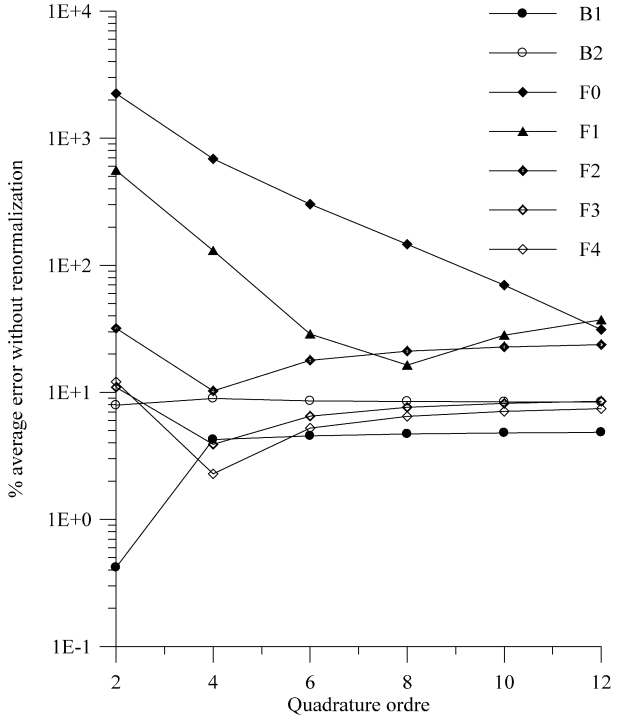

Fig. 5. Percent average error without Mie-phase function renormalization vs quadrature order.

Finally, we can state that the method of Kim is easy to implement and presents the same degree of accuracy as that of Wiscombe. However, the method of least squares stands out in particular by the absence of unrealistic results and the possibility of renormalizing the phase function with the desired accuracy.

In the next section, we set out to analyse the effect of the phase function renormalization on the total modeling of the radiative heat transfer within a rectangular cavity where non-isotropic scattering is taken into account.

4. Radiative pattern in a 2-D rectangular enclosure

4.1. The modified discrete transfer (MDT) method

The present work purports to adapt an original version of the MDT method applied to a parallelepipedic geometry [8] for the analysis of the radiative transfer within a rectangular configuration which confines a semi-transparent medium (STM), gray, emitting, absorbing and anisotropically scattering. Taking account of the radiant intensity angular dependance, we have chosen, for the MDT, the direction set outlined in Section 3.4.

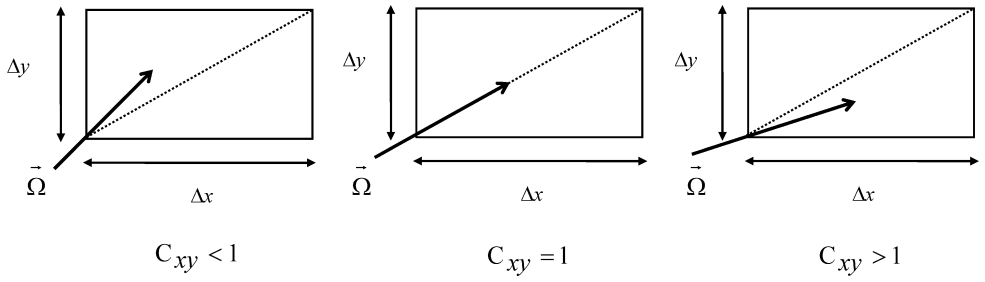

Fig. 6. Representation of different possible cases when a ray crosses a grid cell in the $\vec{\Omega}$ direction.

$$\begin{cases} \mathrm{f(M)} = \mathrm{u}\ \mathrm{f(I)} + (1-\mathrm{u})\ \mathrm{f(I+1)} \\ \mathrm{u} = \dfrac{x(\mathrm{I}+1) - x(\mathrm{M})}{x(\mathrm{I}+1) - x(\mathrm{I})} \end{cases}$$

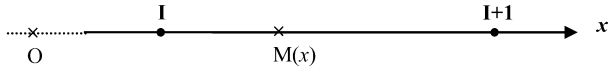

Fig. 7. Definition of the linear interpolation of radiant intensity at point M in terms of adjacent ones.

According to the MDT method, the determination of the radiant intensity field in STM is based on Eqs. (2)–(5). The geometry of the enclosure delimiting this medium determines the choice of the applied interpolation scheme for the calculation of the radiant intensity at the cell entry, the temperature (anisothermal cells) and the scattered radiant intensity at any point located on the path $s_n \to s_{n+1}$. In a Cartesian two-dimensional configuration, Fig. 6 shows three types of possible directions of the radiant intensity crossing a cell where the direction shape parameter $C_{xy} = \frac{\eta \Delta y}{\xi \Delta x}$ characterizes the radiation propagation direction within a rectangular shaped cell $(\Delta x, \Delta y)$ [2].

At the entry of a spatial volume element, radiant intensity has been checked by means of a linear interpolation taking the two adjacent radiant intensities into account (Fig. 7). For each direction type, the interpolation coefficient u $(0 \leqslant u \leqslant 1)$ is depicted on Fig. 8. In each grid cell point, temperature as well as scattered radiation are evaluated, in accordance with those defined in the neighbouring grid cell edges, through the use of a bi-linear interpolation method (Fig. 1), such as [32]

$$f(s) = (1-u)(1-v)f(1) + u(1-v)f(2) + uvf(3) + (1-u)vf(4) \tag{30}$$

where $f = T$ or J_j and (u, v) are the interpolation coefficients defined in $[0, 1]$ that depend on the direction and geometric shape of the considered grid cell. These coefficients are provided in Fig. 9 for each direction type where s represents the distance coordinate between the entry point to a grid cell and the calculation point M. Thus, a given direction is perfectly defined with the direction type (1.8) and the direction number within an octant unit radius sphere.

The assessment of the radiant intensities with the MDT method occurs only at the nodes of each grid cell. Radiation flux and source are then evaluated at these nodes using Eqs. (7)–(9). This avoids averaging the control volume center intensity in accordance with the control volume boundary values. In combined heat transfer processes including radiation and other modes of heat transfer, such as conduction [14] and convection, a displaced grid used for finite-difference or finite volume techniques is considered so that the previous nodes are placed in the center of each control volume.

4.2. Validation of the computer code

In this section, three test problems frequently used in the literature are considered in order to test the possibilities of the calculation program that takes into account various medium and boundary conditions and to choose the adequate spatial and angular discretizations following the comparison with available data. The enclosure is a unit length square shaped geometry with black walls, except for the last test case, containing a semi-transparent and gray medium with a unit optical thickness.

Fig. 10 refers to the case where the medium is purely absorbing with a dimensionless emitted radiative energy and cold walls [33]. By refining the grid cell sizes from 5×5 to 21×21 control volumes (Fig. 10(a)), one notices an improvement in the result accuracy ($n = 6$). The case of 11×11 volume element grid is used for various orders of angular discretization. According to Fig. 10(b) and to tests order 8, which computes 40 intensities over the hemisphere, seems to be the most suitable. The choice of a refined grid carried a slight improvement and increased time calculation. In the following two test cases, a 11×11 spatial grid mesh and $n = 8$ will be adopted. We consider a rectangular enclosure where the top and two side walls are cold while the bottom wall is kept uniformly hot (unit emissive power). The medium is absorbing, emitting and at the radiative equilibrium. The predicted results given on Fig. 11(a), appear to compare well with the exact solution provided by Razzaque et al. [34] for the optically thin and thick limits as well as for a moderate optical thickness value. The last benchmark case involves a cavity, with gray walls of which three are cold and one is hot (unit emissive power), containing an emitting and isotropic scattering medium. Fig. 11(b) shows the profiles of the hot boundary radiative flux for various values of the wall emissivity ε. The comparison gives an excellent agreement with the predictions based on the Hottel zonal method [35] which were successfully used for radiative heat transfer evaluation in practical engineering processes.

The following section focuses on the effect of the studied renormalization phase function methods on the radiative behaviour of a purely scattering–anisotropic radiatively active medium. The MDT solutions will be presented with a much finer spatial and angular discretizations to be used as reference (21×21 element grid, $n = 12$).

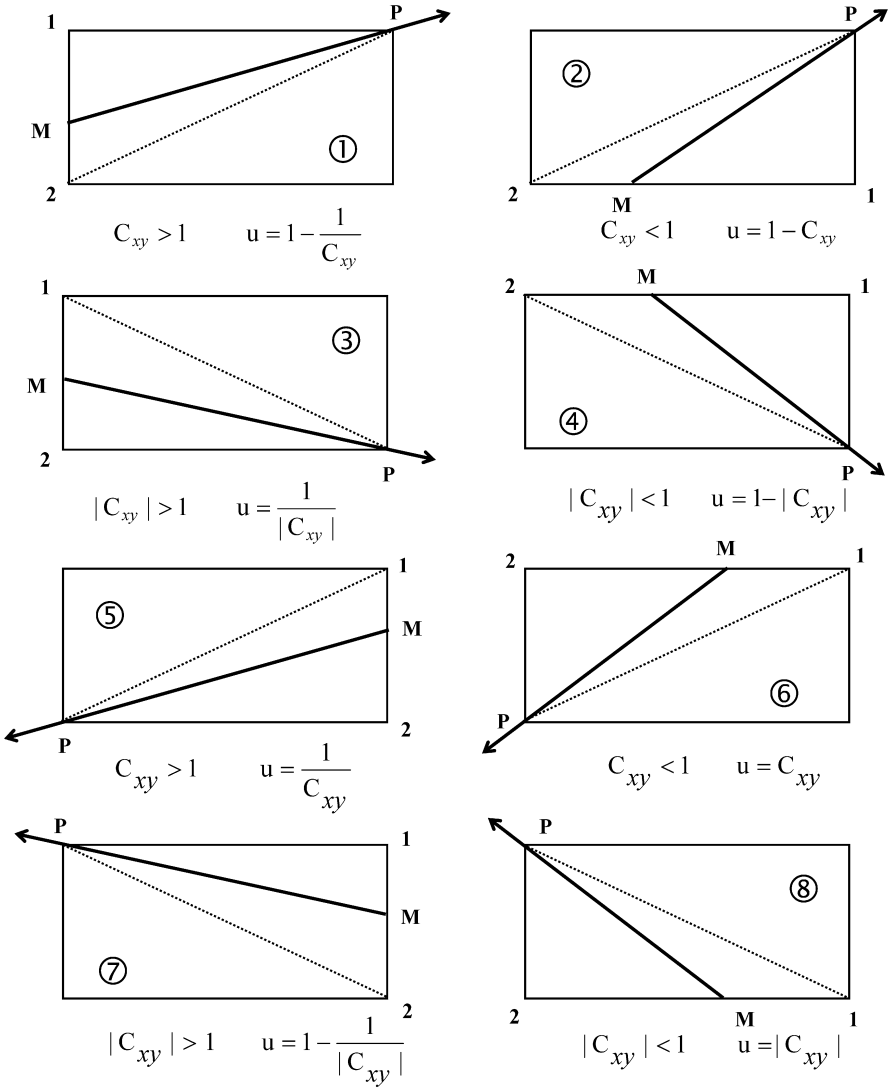

Fig. 8. Presentation of the coefficient u of linear interpolation of radiant intensity for each direction type.

4.3. Comparison between the phase function renormalization methods

In this part, radiant heat transfer within a semi-transparent medium (STM) purely anisotropic scattering ($\beta = \sigma_s = 1\ \mathrm{m}^{-1}$) and confined in a black walled rectangular cavity with unit length is simulated. The wall $y = 0$ is assigned to emissive power of unity (hot wall) whereas the three other walls are cold. The considered phase functions are those studied by Mie: B1, B2, F0, F1, F2, F3 and F4 (Fig. 2). The results suggested by Kim and Lee [10], used as the benchmark, consider the functions B1, B2, F1 and F2 and are obtained by using the discrete ordinates method with classical S-14 quadratures (112 directions) and a Tchebycheff spatial grid of 26×26 volume elements where nodes are tightened in the vicinity of the walls and more spaced when marching towards the central core. For all the phase functions considered renormalization was performed by using Kim's method described in Section 3.2. Our results for the Mie-functions F0, F3 and F4 are provided without comparison since, to our knowledge, these functions were not considered in the present problem. The interested researcher is referred to the work of Kim [12] to obtain the tabulated data for the S-14 predictions used here for comparison.

The calculation of the radiant heat flux and temperatures within the radiating medium follows an iterative process. The solution procedure is considered as converging when the following criterion is satisfied:

$$\left|\frac{U^p - U^{p-1}}{U^p}\right| \leqslant 10^{-4} \quad U = Q \text{ or } T \tag{31}$$

Fig. 12 represents the profiles of the wall radiative flux at the hot surface. We have adopted the same order of magnitude of the average error for the renormalized phase functions by the least squares and Wiscombe methods. The phase functions presenting a large forward scattered component tend to increase the wall radiative flux at the hot wall (F0, F1, F2, F3 and F4) whereas those having a scattering backward directed peak tend to decrease it (B1 and B2). This was predictable since the thermal radiation is directed from the hot surface towards the cavity core.

By examining the profiles of the net radiative and incident fluxes, for different phase functions on the median plane

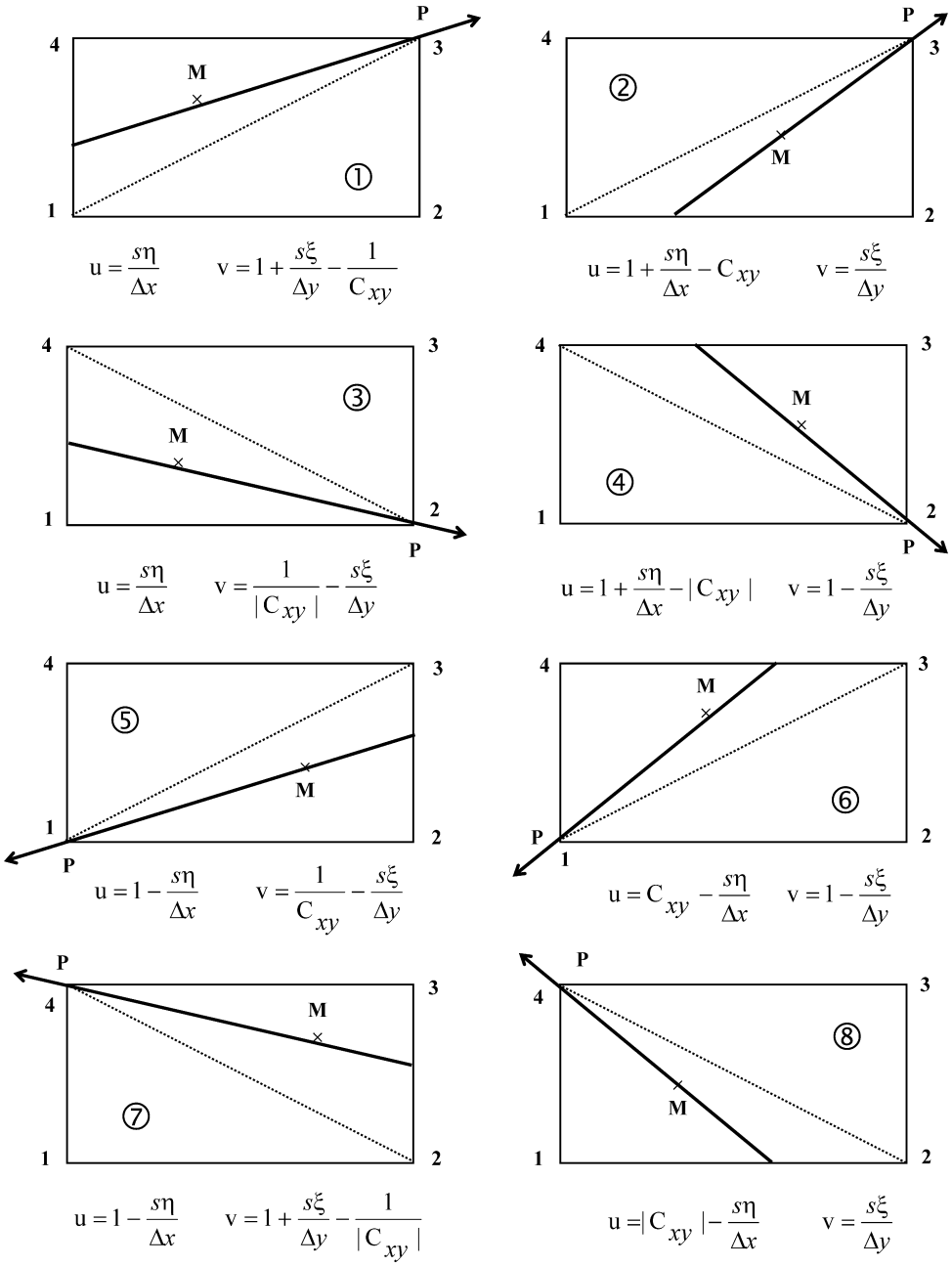

Fig. 9. Presentation of the bilinear interpolation coefficients (u, v) of temperature and scattered radiation for each direction type.

$x = 0.5$ m, we can state that they are not very influenced by the choice of the renormalization method. This can be explained by the symmetry of the medium boundary conditions. It is also noted that for the quadrature sets of order 4 and 6 (functions B1 and B2), the profiles of the net radiative and incident fluxes in the medium presented a wiggling behaviour due to the problem of violating the continuous property of the control angle. Further details about this phenomenon, known as ray effect, can be provided in the literature [6,36,37]. These oscillations are less pronounced if one adopts orders of angular discretization going from $n = 8$ up to 12.

As shown in Table 1 and Fig. 12, the hot wall flux values are for all phase functions accurately predicted when using either the MDT method, associated with the least squares technique, or the scaled isotropic scheme. The maximum error from the S-14 solutions is 3% for the Mie-phase functions B1, B2, F1 and F2. Kim and Lee [11] and Guo and Maruyama [20] have found the equivalent isotropic problem solutions sufficiently accurate by comparison with the anisotropic predictions. More recently, for a one dimensional steady state radiative heat transfer, Tagne and Baillis [17] have shown that the isotropic assumption was accurate for both highly and weakly purely scattering medium and less accurate for thick absorbing–scattering material and forward, backward or forward–backward scattering. Tests have shown that the deviation between the results given by the least squares and the Wiscombe methods is more important for forward radiation scattering functions and for a weak order of angular discretization. Thus, this difference can attain 7% for

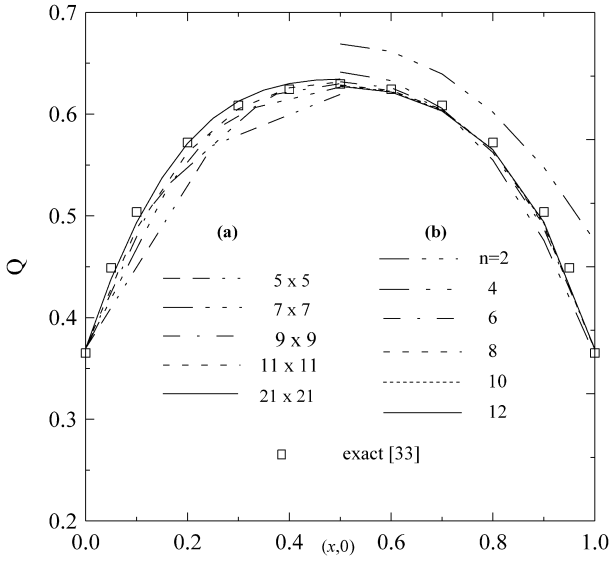

Fig. 10. Spatial grid size (a) and angular discretization (b) effects on the radiative heat flux at one of the cold walls.

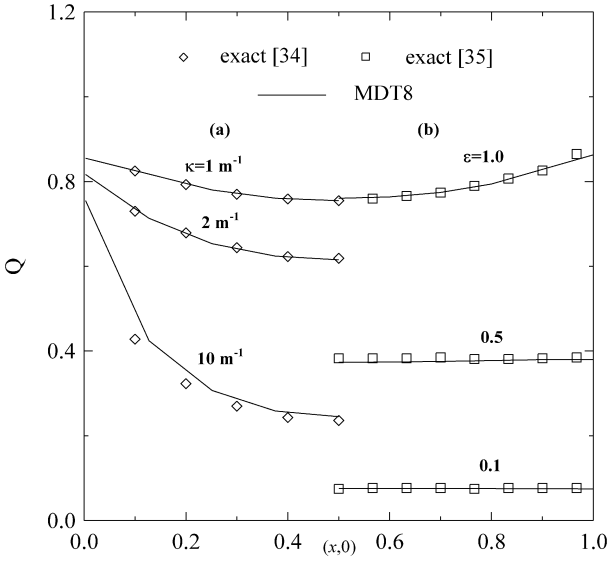

Fig. 11. Optical thickness and wall emissivity effects on the hot walled radiative heat flux (a) $\varepsilon = 1$; $\sigma_s = 0$ (b) $\sigma_s = 1\ \mathrm{m}^{-1}$; $\kappa = 0\ \mathrm{m}^{-1}$.

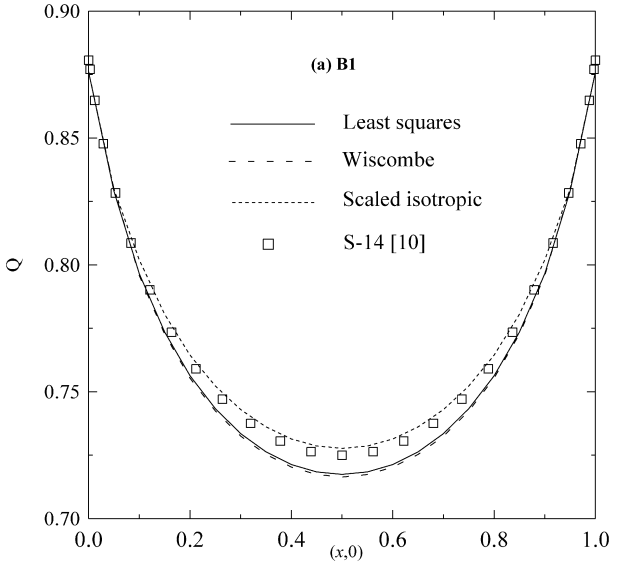

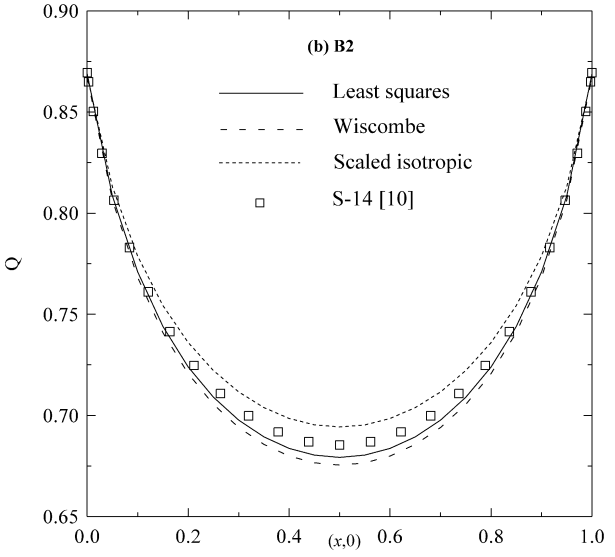

Fig. 12. The hot wall radiative flux profiles for various Mie-phase functions renormalized by using the least squares and Wiscombe methods ($\sigma_s = 1\ \mathrm{m}^{-1}$).

F0, F1 and F2 functions. This can be explained by the fact that the number of terms $\Phi^*_{i,i}$ (incident direction corresponds to that of scattering: $\Psi = 0$) becomes less significant in front of the other terms when the number of discrete ordinates increases. In fact, the variation observed between the results of the two renormalization techniques of the phase function (Wiscombe and least squares) is due to the difference in values occupying the diagonal $\Phi^*_{i,i}$ of the matrix $[\Phi^*]$ since the considered phase function were renormalized by the two methods with the same precision. The comparison between our results and those obtained by the discrete ordinates approximation S-14 (112 directions) have shown the particular interest that the least squares technique presents for renormalizing the phase function. The latter makes it possible to bear the shortcoming of the unrealistic values $\Phi^*_{i,i}$ observed if one adopts the Kim or Wiscombe methods. It is noticed that the various terms of the matrix associated to the renormalized phase function $[\Phi^*]$ must be controlled since negative values due to cumulative errors could take place. In this case, one will be able to remove this negativity by requiring these terms to be positive.

5. Conclusion

A numerical study made it possible to investigate, in a two-dimensional rectangular geometry, the radiative transfer within a semi-transparent, gray, absorbing, emitting and anisotropically scattering medium. The method providing the solutions of the radiative transfer equation (RTE) is based on a new formulation of the modified discrete transfer (MDT) method applied to the case of a 3-D rectangular system [8]. A bilinear interpolation of the temperature as well as of the scattered radiant intensity within a grid cell proved to be necessary in order

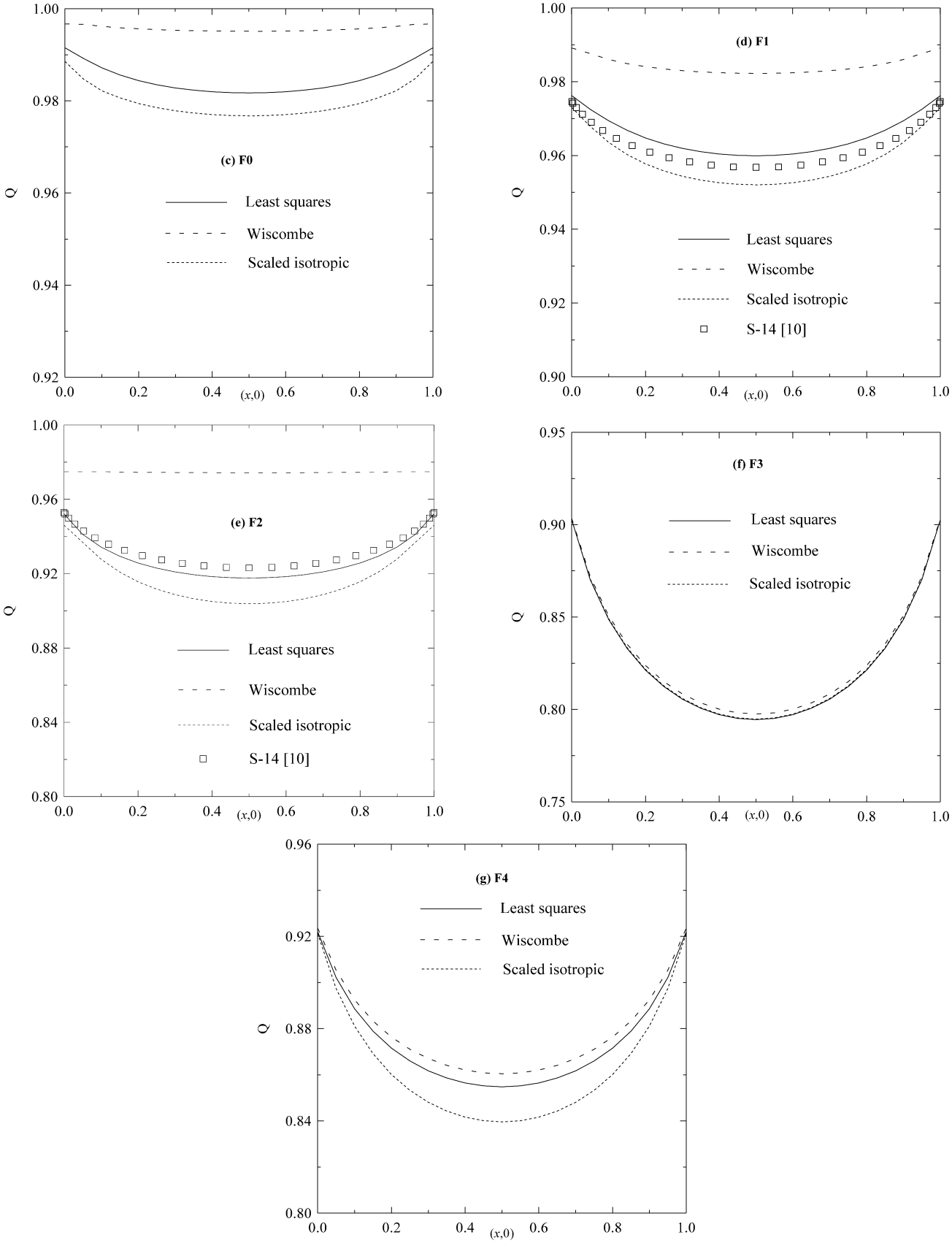

Fig. 12. (*Continued*.)

to cure the drawback of negative radiant intensities occurring when the Cumber linear profile [9] is implemented with a first sharp netting.

By analysing the effect of the renormalization methods of the scattering phase function suggested by Kim, Wiscombe and the least squares technique on the modeling of the radiative transport in a STM containing scattering particles, we have shown that deviation between results given by these methods depends on the angular representation of the scattered radiation (Mie-functions: F0, F1, F2, F3, F4, B1 and B2) and the directional grid size ($n = 2, \ldots, 12$). Kim's method is easier to implement and accomplishes the same degree of accuracy as the one due to Wiscombe. The least squares method offers real prospects since it stands out by the absence of unrealistic values on the diagonal of the matrix assigned to the renormalized phase function and by its ability to renormalize the phase function with the desired accuracy.

For the fully symmetric moment matching technique mentioned previously a data base has been performed involving the correction coefficients of the Mie-phase functions (B1, B2, F0, F1, F2, F3, and F4) using the methods of Kim and Wiscombe and the matrices assigned to each phase function renormalized with the least squares technique. Once assessed, this data base can readily be used with a radiation solver. It is to be noted that the implemented computing code is sufficiently flexible to treat other representations of the scattered radiation not under consideration in this study.

Further stages in this work will consist in considering combined heat transfer modes in enclosures submitted to various thermo-radiative boundary conditions in order to check the suitable phase function renormalization method that provides the best compromise between accuracy and CPU computational time.

References

[1] D. Joseph, M. El Hafi, R. Fournier, B. Cuenot, Comparison of three spatial differencing schemes in discrete ordinates method using three-dimensional unstructured meshes, Int. J. Thermal Sci. 44 (2005) 851–864.

[2] J.C. Chai, S.V. Patankar, H.S. Lee, Evaluation of spatial differencing practices for the discrete-ordinates method, J. Thermophys. Heat Transfer 8 (1994) 140–144.

[3] B.-T. Liou, C.-Y. Wu, Ray effecting the discrete ordinate solution for surface radiation exchange, Int. J. Heat Mass Transfer 32 (1997) 271–275.

[4] M.A. Ramankutty, A.L. Crosbie, Modified discrete ordinates solution of radiative transfer in three-dimensional rectangular enclosures, J. Quant. Spectrosc. Radiat. Transfer 60 (1998) 103–134.

[5] M. Sakami, A. Charette, V. Le Dez, Radiative heat transfer in three-dimensional enclosures of complex geometry by using the discrete ordinates method, J. Quant. Spectrosc. Radiat. Transfer 59 (1998) 117–136.

[6] P.J. Coelho, The role of ray effects and false scattering on the accuracy of the standard and modified discrete ordinates method, J. Quant. Spectrosc. Radiat. Transfer 73 (2002) 231–238.

[7] N.-R. Ou, C.-Y. Wu, Simultaneous estimation of extinction coefficient distribution, scattering albedo and phase function of a two-dimensional medium, Int. J. Heat Mass Transfer 45 (2002) 4663–4674.

[8] H. Farhat, M.-S. Radhouani, Etude tridimensionnelle du transfert radiatif dans un milieu semi-transparent diffusant anisotrope par la méthode des transferts discrets modifiée, Rev. Gén. Therm. 36 (1997) 330–344.

[9] P.S. Cumber, Improvements to the discrete transfer method of calculating radiative heat transfer, Int. J. Heat Mass Transfer 38 (1995) 2251–2258.

[10] T.-K. Kim, H.S. Lee, Effect of anisotropic scattering on radiative heat transfer in two-dimensional rectangular enclosures, Int. J. Heat Mass Transfer 31 (1988) 1711–1721.

[11] T.-K. Kim, H.S. Lee, Scaled isotropic results for two-dimensional anisotropic scattering media, J. Heat Transfer 112 (1990) 721–727.

[12] T.K. Kim, Radiation and combined mode heat transfer analysis in absorbing, emitting and Mie-anisotropic scattering media using the S-N discrete ordinates method, PhD thesis, Faculty of the Graduate School of the University of Minnesota, 1990.

[13] H.S. Lee, R.O. Buckius, Scaling anisotropic scattering in radiation heat transfer for a planar medium, ASME J. Heat Transfer 104 (1982) 68–75.

[14] M.N. Özisik, Radiative Transfer and Interactions with Conduction and Convection, John Wiley and Sons, New York, 1973.

[15] W.J. Wiscombe, On initialisation, error and flux conservation in the doubling method, J. Quant. Spectrosc. Radiat. Transfer 18 (1976) 637–658.

[16] N. Berour, D. Lacroix, P. Boulet, G. Jeandel, Radiative and conductive heat transfer in a nongrey semitransparent medium. Application to fire protection curtains, J. Quant. Spectrosc. Radiat. Transfer 86 (2004) 9–30.

[17] H.T.K. Tagne, D. Baillis, Isotropic scaling limits for one dimensional radiative heat transfer with collimated incidence, J. Quant. Spectrosc. Radiat. Transfer 93 (2005) 103–113.

[18] W.J. Wiscombe, The delta-M method: Rapid yet accurate radiative flux calculations for strongly asymmetric phase functions, J. Atmos. Sci. 34 (1977) 1408–1422.

[19] B.H. McKellar, M.A. Box, The scaling group of the radiative transfer equation, J. Atmos. Sci. 38 (1981) 1063–1068.

[20] Z. Guo, S. Maruyama, Scaling anisotropic scattering in radiative transfer in three-dimensional nonhomogeneous media, Int. Comm. Heat Mass Transfer 26 (1999) 997–1007.

[21] J.S. Truelove, Discrete ordinates solutions of the radiation transport equation, J. Heat Transfer 109 (1987) 1048–1051.

[22] R. Siegel, J.R. Howell, Thermal Radiation Heat Transfer, second ed., Hemisphere, New York, 1981.

[23] C. Brezinski, Algorithmes d'accélération de la convergence. Etude numérique. Collection langages et algorithmes de l'informatique, Editions Technip, Paris, 1978.

[24] M.E. Larsen, J.R. Howell, Least-squares smoothing of direct-exchange areas in zonal analysis, J. Heat Transfer 108 (1986) 239–242.

[25] R. Méchi, H. Farhat, K. Halouani, M.-S. Radhouani, Modélisation des transferts radiatifs dans un incinérateur des émissions polluantes de la pyrolyse du bois, Int. J. Thermal Sci. 43 (2004) 697–708.

[26] M.E. Larsen, The exchange factor method: An alternative zonal formulation for analysis of radiating enclosures containing participating media, PhD dissertation, University of Texas, Austin, 1983.

[27] M.E. Larsen, J.R. Howell, The exchange factor method: An alternative basis for zonal analysis of radiating enclosures, J. Heat Transfer 107 (1985) 936–942.

[28] B.G. Carlson, K.D. Lathrop, Transport theory: The method of discrete ordinates, in: H. Greenspan, C.N. Kelber, D. Okrent (Eds.), Computing Methods in Reactor Physics, Gordon and Breach, New York, 1968, pp. 171–266.

[29] K.D. Lathrop, B.G. Carlson, Discrete ordinates angular quadrature of the neutron transport equation, Los Alamos Scientific Laboratory, Report LASL-3186, 1965.

[30] W.A. Fiveland, Three-dimensional heat transfer solutions by the discrete ordinates method, in: Fundamentals and Applications of Radiation Heat Transfer, ASME HTD, New York, 1987, pp. 9–18.

[31] J.S. Truelove, Three-dimensional radiation in absorbing-emitting-scattering media using the discrete ordinates approximation, J. Quant. Spectrosc. Radiat. Transfer 39 (1988) 27–31.

[32] W.H. Press, S.A. Teukolsky, W.T. Vetterling, B.P. Flannery, Numerical recipes in C, in: The Art of Scientific Computing, second ed., Cambridge, 1992.

[33] J. Gibb, Analytic solution to a two-dimensional Cartesian geometry, Private communication, March 1977.

[34] M.M. Razzaque, D.E. Klein, J.R. Howell, Finite element solution of radiative heat transfer in a two-dimensional rectangular enclosure with grey participatin medium, J. Heat Transfer 105 (1983) 933–936.

[35] A. Ratzel, J.R. Howell, Two-dimensional radiation in absorbing-emitting-scattering media using the P–N approximation, ASME Paper, n° 82-HT-19, 1982.

[36] J.C. Chai, H.S. Lee, S.V. Patankar, Ray effect and false scattering in the discrete ordinates method, Numer. Heat Transfer (Part B) 24 (1993) 373–389.

[37] M. Sakami, A. Charette, Application of a modified discrete ordinates method to two-dimensional enclosures of irregular geometry, J. Quant. Spectrosc. Radiat. Transfer 59 (1998) 117–136.